Permeation and gating of α1 glycine-gated channels expressed at low and high density in *Xenopus* oocyte

Mohammed Maammar, Jean-Luc Rodeau, Omar Taleb*

Laboratoire de Neurobiologie Cellulaire, UPR CNRS 9009, 5 rue Blaise Pascal, F- 67084 Strasbourg, France

Received 25 July 1997

Abstract When a high density of α1-subunit glycine receptor (GlyR) is expressed in *Xenopus* oocytes, two populations of channels can be distinguished according to their apparent affinity for glycine which differs 5- to 6-fold. To compare the open pore diameter of these channels, the relative permeability of formate with respect to chloride ($P_{formate}/P_{Cl}$) was determined in bionic conditions. For the low-affinity GlyR $P_{formate}/P_{Cl}$ was comparable to that reported for glycine-gated channels in cultured spinal cord and hippocampal neurons. In contrast, the high-affinity GlyR had a 56% larger $P_{formate}/P_{Cl}$. In addition, the open probability of the channels was differentially sensitive to voltage. These results show that the high expression of α1 GlyR resulted in two populations of GlyR which differed not only in the affinity to agonists but also in permeation and gating mechanisms.

Key words: Glycine-gated channel; α1-Subunit formed homo-oligomeric channel; Anion channel

1. Introduction

Glycine is the major inhibitory neurotransmitter in the spinal cord where it activates a chloride permeant channel. Constitutive subunits of this channel have been purified: 2 pore-forming subunits of 48 kDa (α) and 58 kDa (β), respectively, and a third cytoplasmic 93 kDa (gephyrin) subunit [1]. The structure of the native GlyR in spinal cord neurons was suggested to be pentameric [2] with an $\alpha_3\beta_2$ stoichiometry. A variety of channel types have been developed in expression systems: homomeric channels formed by expression of only α-subunits [3–6] and probably heteromeric channels formed by injection of poly(A)$^+$ RNA of spinal cord [3] or by co-expression of the cloned α- and β-subunits [7–9]. Functional properties of expressed channels also suggest a pentameric stoichiometry [6]. When compared to native channels, expressed channels display a similar exquisite sensitivity to the competitive antagonist strychnine and are activated with decreasing apparent affinity, by glycine, β-alanine and taurine. A consistent discrepancy is nevertheless that expressed receptor channels are, in most cases, low-affinity receptors as compared to native channels which display a 5- to 10-fold higher apparent affinity for the agonist [3–5,10,11]. Expressed channels with an exceptionally high apparent affinity for their agonists were obtained by direct nuclear injection of large amounts of α1 cDNA and subsequent expression of a large number of glycine receptors [5]. In addition to the usual low-affinity receptors, this protocol yielded a population of high-affinity glycine receptors. Distinct channels may have been processed, considering the high rates of induced channel synthesis. Alternatively, direct interactions between otherwise identical channels may be suggested to occur when very high densities of channels are attained. Whatever the underlying mechanism, the present work was undertaken to examine the permeation and gating characteristics of the two channel populations so as to get some insight as to the functionality of the channel formed in each case.

*Corresponding author. Fax: (33) 388-60-16-64.
E-mail: omar@neurochem.u-strasbg.fr

Abbreviations: EC_{50}, half-maximal effective concentration; GlyR, glycine receptor; GlyR channel, glycine-gated channel

2. Materials and methods

2.1. Expression in Xenopus oocytes

The experimental procedure was as previously described [5]. Briefly, oocytes were mechanically dissociated from pieces of *Xenopus* ovaries kept in Ca-free frog saline solution which was composed of: (in mM) NaCl 100, KCl 2, $MgCl_2$ 1, HEPES 5, pH 7.6 adjusted with NaOH. Mature oocytes were selected and incubated in the same solution containing 1.8 mM $CaCl_2$, for 2–6 h before injection. Plasmid pCis [11] which contained a cDNA insert coding for the human α1 GlyR subunit was diluted in water at a concentration of either 5 or 20 pg/nl which lead to respectively low and high expression levels of GlyR. Oocytes were nuclearly injected with about 10 nl of this plasmid solution. The oocytes were kept at room temperature overnight and then incubated at 10°C for up to 10 days before recording.

2.2. Electrophysiological recordings

Whole-cell currents were recorded from oocytes placed in a linear chamber which yielded solution exchange in a few seconds. The recorded oocyte was continuously superfused with control medium containing (in mM): NaCl 115, KCl 1, $CaCl_2$ 1.8, HEPES 10, pH 7.2 adjusted with NaOH. The ionic current flowing through plasma membrane was measured using a two electrodes high-voltage-driven voltage-clamp setup (WPI voltage follower combined with the CA-100 amplifier and the VF1800 current injection unit from Biologic, Grenoble, France). The recording pipettes were filled with 3 M KCl and had resistances of about 3 and 0.7 MW, respectively, for voltage measurement and current injection. Voltage command and current trace digitization were achieved using the TL-1 Labmaster interface card and pClamp software (Axon Instruments).

In some experiments in addition to the cellular current, the intracellular chloride concentration, $[Cl]_i$, was measured using chloride-sensitive microelectrodes (chloride ion exchanger Corning 477315; mean slope ≅ −54 mV). This was done to monitor the variations of $[Cl]_i$ during glycine application and external chloride substitution with formate ions.

For anion substitution, 108 mM of sodium formate replaced 108 mM of NaCl in the external medium. Solution exchange was performed 2–10 min before glycine application.

In all data presented here the membrane potential was corrected for the liquid junction potential, which did not exceed 5 mV and was determined as previously described [12].

2.3. Analysis

Glycine-induced cellular currents were measured at room temperature (≈20°C) 2–10 days after injection. To obtain the agonist-specific current component, the current measured at a given potential in control condition was systematically subtracted from the current re-

PII S0014-5793(97)00986-1

corded in the presence of the agonist. To determine the instantaneous current (I_{ins}) value after a potential change, the current recorded after peak was extrapolated to the start of the potential step according to a mono-exponential time course. Steady-state current–voltage (I–V) plots were constructed using the mean current values of the last 10 ms of the potential step. Depending on the shape of I–V plots, reversal potentials (V_0) were determined either from a linear regression or from a non-linear fit, using the Boltzmann model for the cellular current (I):

$$I = \frac{g(V-V_0)}{1+\exp[-(V-V_{1/2})/k]}$$

where g, V, $V_{1/2}$ and k refer to the cellular conductance, test potential, potential for half-maximal activation and slope factor, respectively.

On the basis that the washout gave the same reversal potential as the control condition and that in formate condition the reversal potential did not change with time (up to 30 min), it was assumed that the intracellular concentration of formate was null and that chloride was the only permeant anion inside the cell. Direct measurements of $[Cl]_i$ confirmed its constancy during the duration of recordings. The relative permeability $P_{formate}/P_{Cl}$ was hence calculated using the Goldman-Hodgkin-Katz (GHK) equation:

$$V_0 = -\frac{RT}{F}\ln\left(\frac{[Cl]_e + (P_{formate}/P_{Cl})[formate]_e}{[Cl]_i}\right)$$

The subscripts 'i' and 'e' refer to intracellular and extracellular medium, respectively, RT/F has the usual meaning and a value of 25 mV at 20°C. The intracellular chloride concentration $[Cl]_i$ was calculated from the reversal potential obtained in control conditions using the Nernst equation:

$$V_0 = -\frac{RT}{F}\ln\frac{[Cl]_e}{[Cl]_i}$$

The tail current recorded at holding potential $V_h = -40$ mV after various test potentials, V, was analyzed to determine the relative open probability $p_{(V/V_h)}$. For each concentration of agonist (either 50 or 400 μM glycine) $p_{(V/V_h)}$ is equal to the ratio I_{ins}/I_{SS} where I_{ins} is the instantaneous current as described above and I_{SS} is the steady-state current measured at V_h. $p_{(V/V_h)}$ varied as a function of test potential according to a sigmoidal curve and was fitted with the Boltzmann equation:

$$p_{(V/V_h)} = p_{min} + \frac{p_{max}-p_{min}}{1+\exp[zF(V_{1/2}-V)/RT]}$$

The subscripts 'min' and 'max' indicate, respectively, the minimal and maximal limits of open probability change as a function of potential. $V_{1/2}$ and z are the potential of half-maximal activation and the gating charge, respectively.

The results, otherwise indicated, are expressed as mean value ± SEM.

3. Results

Whole-cell currents in oocytes expressing the homo-oligomeric human α1 glycine receptor were recorded in conditions devised to record in isolation the low- and high-affinity GlyRs. By measuring their sensitivity to changes in the membrane potential, the selectivity of the channels to formate rel-

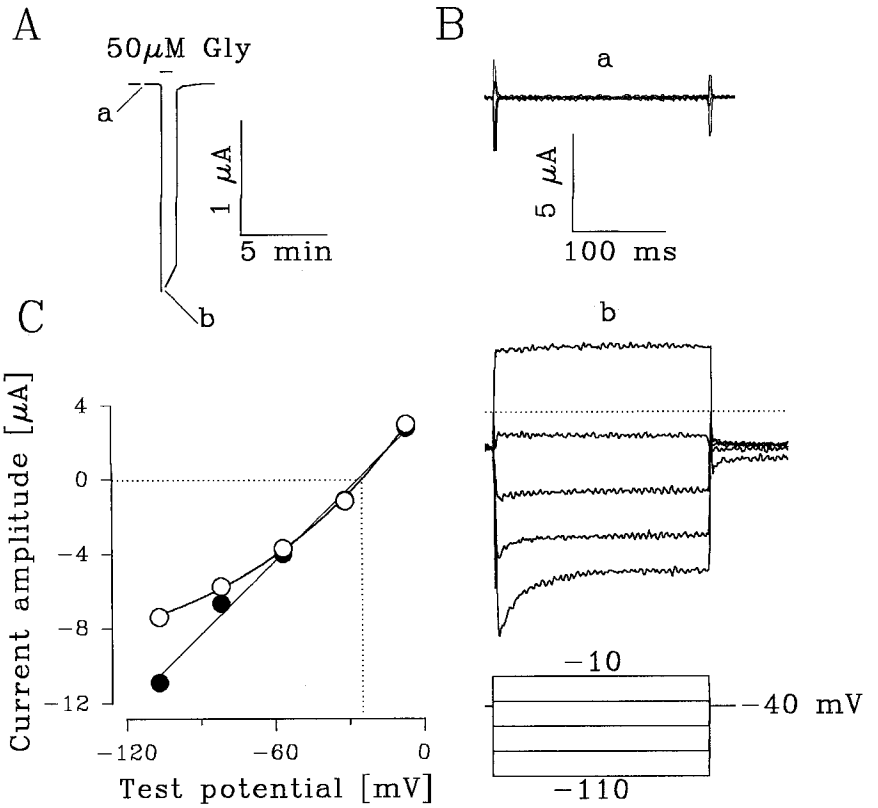

Fig. 1. Glycine-evoked response and its I-V relationship in *Xenopus* oocyte expressing α1 oligo-homomeric GlyR. A: Mean of three successive current responses to a 1 min application of 50 μM glycine recorded from an oocyte injected with 100 pg of α1 cDNA. The holding potential was −40 mV. Interruption of the trace in (a) and (b) indicate the time at which the test pulse protocol was performed. B: Current responses to a series of potential steps (protocol at the bottom) obtained successively before (a) and during (b) glycine application. The traces (Bb) were obtained after subtraction of traces (Ba) in order to eliminate capacitive transients and non-specific current. The dotted line represent the zero current. C: I–V relationship of instantaneous (●) and steady-state (○) currents of traces (Bb). Lines were fitted to data points using linear regression for instantaneous current or the Boltzmann model for steady-state current. Note that the reversal potential was similar in both cases: −26.8 and −25.2 mV respectively for instantaneous and steady-state curves. The latter value is indicated by dotted lines.

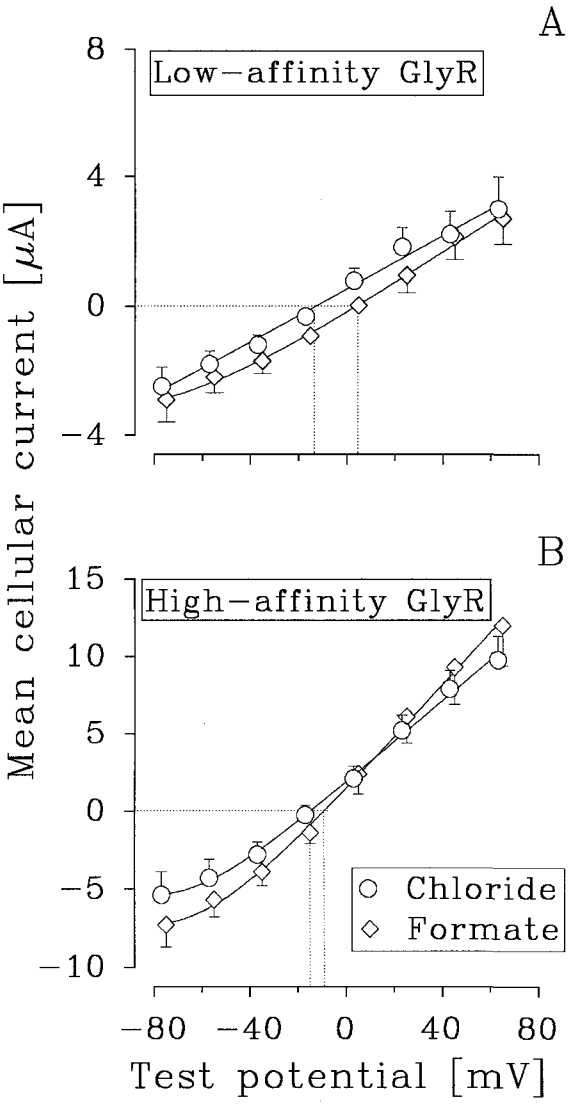

Fig. 2. Whole-cell steady-state *I-V* relationships recorded with low- and high-affinity GlyRs in monoionic (Cl^-, ○) and bionic (formate, ◇) conditions. The low-affinity GlyR was activated in isolation on oocytes showing low expression of the receptor using 400 μM glycine (A). Whereas the high-affinity GlyR was assayed on oocytes with high expression level using 50 μM glycine (B). Data are means of 8 cells from different batches of oocytes; vertical bars represent SEM. Continuous lines were fitted using the Boltzmann equation (see Section 2). Mean values of the reversal potential in Cl^- and formate conditions are indicated by dotted lines and were, respectively, −12.8 ± 3.2 mV and 4.1 ± 2.2 mV for the low-affinity, and −15.0 ± 1.7 mV and −9.3 ± 1.8 mV for the high-affinity. Note that the current in (B) is larger due to the higher density of receptors and that the outward rectification is more pronounced for the high-affinity GlyR.

ative to chloride and the sensitivity of channel opening to voltage were characterized and compared.

3.1. Current–voltage relationship in Cl^- medium

Low- or high-affinity GlyR populations were activated in quasi-isolation using oocytes showing, respectively, low or high GlyR expression and a glycine concentration (400 or 50 μM) close to the corresponding EC_{50} of the two GlyR types.

Fig. 1 shows a typical response obtained during a 1 min application of 50 μM glycine. The responses developed relatively rapidly, and at the agonist concentration applied here, remained stable at the peak value for a few seconds before apparent desensitization of the response was seen. The membrane potential was stepped briefly to different levels ranging from −110 to −10 mV. The response at any potential was biphasic. At the onset of a potential step, the current instantaneously attained a new value and then evolved relatively slowly to a steady-state level with a relaxation time constant which slightly increased with membrane potential: for example it had a mean value of 37.1 ± 7.7 and 28.2 ± 3.8 ms at a test potential of −80 mV, and 79.7 ± 25.8 and 40.2 ± 4.4 ms ($n = 8$) at 20 mV for the low- and high-affinity GlyRs, respectively. Typically the instantaneous *I-V* relation was linear and the steady-state *I–V* relation displayed an outward rectification (Fig. 1C). All of these electrophysiological characteristics are similar to those observed on native somatic channels of cultured spinal cord neurons [10].

The reversal potential of the glycine response was similar for low- and high-affinity GlyR, with no statistically significant difference, and had an average value of −18.1 ± 1.0 mV ($n = 26$). This value was used to estimate the intracellular concentration of Cl^- assuming that no other anionic permeability took place. Thus, in oocytes bathed in a 119.6 mM Cl^- medium, the calculated internal Cl^- concentration was 59.4 ± 2.4 mM ($n = 26$). This was not significantly different from the average value of $[Cl]_i$ directly measured with chloride-sensitive microelectrodes (53.0 ± 9.1 mM; mean ± SD, $n = 4$).

3.2. Selectivity to formate of the low-affinity GlyR channel

The organic anion formate was chosen to calibrate the narrow restriction diameter of the open channel pore, since it has

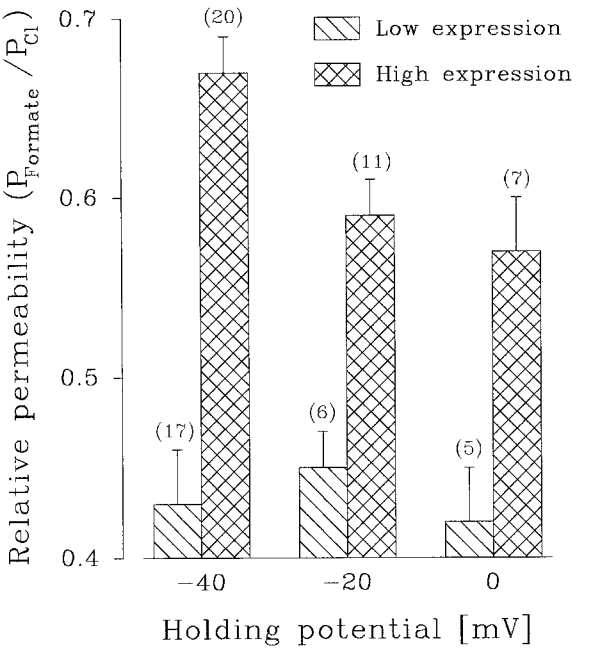

Fig. 3. Permeability ratio of formate relative to Cl^- ($P_{formate}/P_{Cl^-}$) for the low- and high-affinity glycine receptors at holding potentials of −40, −20 and 0 mV. The ratio $P_{formate}/P_{Cl^-}$ was calculated from the reversal potentials obtained from monoionic and bionic conditions using the Goldman-Hodgkin-Katz model (see Section 2). At all holding potentials a highly significant difference was observed between low- and high-affinity conditions (Student's *t* test; $p < 0.001$).

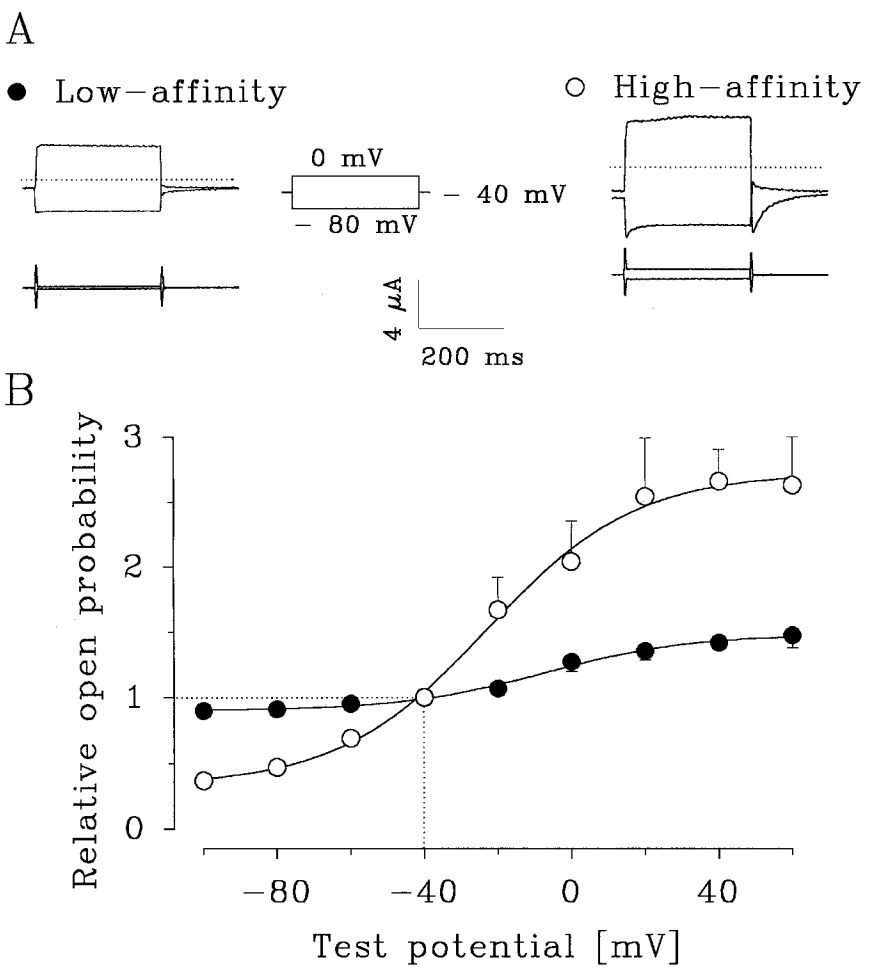

Fig. 4. Open probability of low- and high-affinity GlyR channel. A: Typical traces of current responses to the step potential protocol (middle traces) obtained in control (bottom traces) or during glycine application at a concentration of 400 μM (left upper traces) or 50 μM (right upper traces). Traces given in the presence of the agonist were obtained after subtraction of the respective control. The dotted lines indicate the zero current level. B: Relationship between relative open probability and test potential for low- (●) and high-affinity (○) glycine receptors. The instantaneous current at −40 mV after each test potential, I_{ins}, was obtained from a mono-exponential fit of the tail current (A). To normalize data, the relative open probability at a given test potential was calculated as the ratio of I_{ins} over the steady-state current at −40 mV. Symbols show means of 6–13 cells and vertical bars represent SEM. The continuous lines are fits to the Boltzmann model.

a larger molecular diameter than chloride and its passage through the channel depends essentially on friction forces [13]. Importantly, in our conditions formate had very limited if no diffusion through the plasma membrane as compared to other larger organic anions as propionate for example (data not shown). Indeed, the reversal potential in formate condition did not change with time (up to 30 min) and after return to the Cl^- medium it was identical to that obtained in control (data not shown). Determination of reversal potential was systematically performed for each oocyte successively in a Cl^--containing solution then in a formate-containing solution in which 108 mM Cl^- was substituted for. In these experiments the membrane potential was held at −40 mV.

Fig. 2A illustrates the mean *I-V* relationship obtained for different oocytes where GlyR was expressed at low levels (see Section 2) and activated by application of 400 μM glycine. It can be readily seen that the reversal potential in low Cl^- formate-containing medium was shifted to more depolarized potentials with a shift amplitude ranging from 10 to 26 mV. The mean shift value was 19.1 ± 1.6 mV ($n = 17$). Statistical comparison of the *I–V* relations observed in Cl^- and formate conditions, respectively, was performed by analyzing the residual variance of the fit by the Boltzmann equation. A highly significant improvement of the fit ($p < 0.0001$) was obtained when the reversal potential was given a different value for each group (rather than a common value). The same analysis performed for the other parameters of the *I–V* curves (g, $V_{1/2}$ and k) showed no difference between chloride and formate conditions: the difference between the curves is thus mainly due to a shift in the reversal potential.

3.3. Selectivity to formate of the high-affinity GlyR channel

Similar experiments were carried with oocytes expressing a high level of α1 GlyR (Fig. 2B), applying this time 50 μM glycine. For all the cells in this condition the reversal potential shifted systematically to the right, when switching from Cl^-- to formate-containing medium. However, the amplitude of the shift was small and ranged between 4 and 16 mV, which gave a mean value of 9.2 ± 0.7 mV ($n = 20$). Statistical comparison of the two groups using either common or distinct parameters (V_0, g, $V_{1/2}$ or k) showed a significant difference only for V_0.

Obviously the potential shift for the low-affinity GlyR had

a mean value which was twice of that for the high-affinity GlyR. This difference was highly significant (Student's t test, $p < 0.0001$).

3.4. The origin of the difference in potential shift between low- and high-affinity GlyRs

The smaller amplitude of potential shift observed for the high-affinity GlyR may result from a decrease of $[Cl]_i$ after the exchange of external Cl^- ions for formate ions. This may occur more markedly in oocytes showing a high expression of GlyR, since high expression may increase the oocytes endogenous Cl^- permeability [14]. To check this point two different methods were used: reducing the driving force exerted on Cl^- ions and measuring $[Cl]_i$ during Cl^- substitution by formate.

In a set of experiments the membrane potential of the oocyte was held successively to holding potentials of −40, −20 and 0 mV and small potential steps were applied around the reversal potential (between −30 and 10 mV). For the low-affinity GlyR the data showed a relatively constant potential shift. Mean values of 17.7 ± 0.8 ($n = 6$) and 18.8 ± 1.4 ($n = 5$) were obtained respectively at −20 and 0 mV, not significantly different from -19.1 ± 1.6 mV observed at −40 mV (1-way analysis of variance (ANOVA), $p = 0.85$). In contrast, for the high-affinity GlyR the potential shift slightly increased with holding potential. The mean values obtained at −20 and 0 mV were 11.9 ± 0.7 ($n = 11$) and 12.6 ± 1.0 ($n = 7$), respectively. One-way ANOVA showed a significant effect of holding potential ($p = 0.012$), the value of the shift at −40 mV (9.2 ± 0.7 mV) differing significantly from the two others. Interestingly, the potential shift of the low-affinity GlyR showed a highly significant difference with that of the high-affinity GlyR at all holding potentials, even at 0 mV.

In other experiments $[Cl]_i$ was measured with chloride-sensitive microelectrodes. Since the changes of the potential shift with V_h were seen only with the high-affinity GlyR, $[Cl]_i$ was measured in conditions where cytosolic Cl^- ions extrusion, if any, would be maximal in the previous experiments, i.e. a high expression of GlyR and a holding potential of −40 mV. Since the Cl^- ion exchanger is also sensitive to formate ions, external Cl^- ions were replaced by gluconate ions which were not detected by the Cl^--sensitive electrode. Perfusing the cells with a gluconate-containing medium for up to 15 min did not induce any detectable change in $[Cl]_i$. Similarly no changes could be recorded when replacing Cl^- by formate. However, when applying 50 μM glycine a slow decrease of $[Cl]_i$ could be observed which reached about 2 mM, at the peak of the agonist-induced response (current amplitude ≅ 1 μA). This $[Cl]_i$ change recovered within 5 min after washout of the agonist. Thus among the factors liable to induce $[Cl]_i$ changes in our conditions, Cl^- ions fluxes through GlyR channels are potentially more important than endogenous oocyte Cl^- permeabilities.

Altogether this means that the significant difference in potential shift observed between low- and high-affinity GlyR must be due to changes in the selectivity of the GlyR channel.

3.5. Relative permeability for formate

The permeability ratio for formate relative to chloride was calculated using the GHK model (see Section 2) for each cell. As expected from the reversal potential in the presence of formate, for the low affinity GlyR $P_{formate}/P_{Cl}$ was significantly smaller than that obtained for the high-affinity GlyR (Fig. 3). For the low-affinity GlyR identical $P_{formate}/P_{Cl}$ ratios were obtained for the different holding potential tested. Mean values of 0.43 ± 0.03 ($n = 17$), 0.45 ± 0.02 ($n = 6$) and 0.42 ± 0.03 ($n = 5$) were obtained at −40, −20 and 0 mV, respectively. This value is close to that reported for the α1 GlyR heterologously expressed in a mammalian cell line [9] and the native CNS GlyR [13,15]. In contrast for the $P_{formate}/P_{Cl}$ ratio of the high-affinity GlyR mean values of 0.67 ± 0.02 ($n = 20$), 0.59 ± 0.02 ($n = 11$) and 0.57 ± 0.03 ($n = 7$) were obtained at holding potentials of −40, −20 and 0 mV, respectively. As expected from the analysis of reversal potentials, holding potential was found to have a significant effect on the permeability ratio of the high-affinity GlyR (1-way ANOVA, $p = 0.008$).

These data lead to the conclusion that the bore diameter of the channel at its narrow restriction was much larger for the high-affinity GlyR population than for the low-affinity GlyR.

3.6. Voltage sensitivity of the response

As seen above the glycine response observed after a potential change increased to a steady-state level. Moreover, the time constant of the relaxing current induced by the step potential increased and nearly doubled over a 100 mV potential change (see above). This probably corresponds to changes in channel gating corresponding to an increase of the open time and/or open probability of the channel.

The latter was estimated at the holding potential of −40 mV by analyzing the deactivation relaxation of the current after various test potentials (see Section 2). Generally, $p_{(V/V_h)}$ was well described with a Boltzmann distribution with a similar apparent gating valence for both receptor populations: z was 1.3 ± 0.2 and 1.2 ± 0.2 ($n = 8$) respectively for the low- and high-affinity GlyRs f4(Fig. 4). However, significant differences between low- and high-affinity GlyRs were seen in the minimum (p_{min}) and maximum (p_{max}) limits of the change in the relative open probability. The range was smaller for the low-affinity GlyR. Mean values of 0.90 ± 0.02 for p_{min} and 1.48 ± 0.03 for p_{max} were obtained for the low-affinity GlyR. In contrast, for the high-affinity GlyR p_{min} and p_{max} had mean values of 0.33 ± 0.08 and 2.73 ± 0.07, respectively. The $V_{1/2}$ also changed and was -6.7 ± 3.4 and -22.6 ± 2.5 mV, respectively, for the low- and high-affinity GlyRs.

4. Discussion

In this study, we used cDNA injection into *Xenopus* oocyte nuclei to generate GlyRs over a wide range of expression levels. The efficiency of the α1 GlyR expression allowed to compare receptor properties when changing their densities at the level of the plasma membrane with a factor comparable to that of synaptic versus extra-synaptic receptors. At high density a high-affinity GlyR subpopulation appears which has a different pharmacological profile [5]. The present study shows that the high-affinity GlyRs are associated with anion channels of different permeation and gating properties. Indeed, when expressed at low density, homomeric GlyRs were comparable (in terms of relative permeability to formate ions) to the native heteromeric GlyRs of the adult mammalian cultured spinal cord neurons [13], although, they differed in terms of affinity for agonists. At a variance the high-affinity

GlyR population, with the same EC_{50} as native channels, showed a highly significative increase of the relative permeability for formate. The relative permeability for formate was estimated here with assumptions about the cytosolic chloride concentration and the minor participation of other intracellular anions. We assumed that chloride was the only anion charge carrier. This assumption is validated by the fact that the calculated intracellular chloride concentration was found to be not significantly different from that directly measured with chloride-sensitive microelectrodes. Its value was slightly higher but comparable to that measured with intracellular chloride-sensitive electrodes on urodele oocytes [16]. Furthermore no change in $[Cl]_i$ was detected with intracellular electrodes during substitution of external chloride. This and the fact that the reversal potential after washout of formate was identical to control, confirms that indeed there was no sizable participation of other cytosolic anions in our conditions. In any case, the difference in relative permeability between low- and high-affinity GlyRs is observed whatever the holding potential (Fig. 3), even when the driving force exerted on Cl^- ions is minimized at depolarized potentials.

The change in permeation observed at high receptor density probably reflects a change in the narrow constriction of the open channel pore. Many arguments are in favor of a pentameric conserved structure for the receptor channel superfamily. This seems to be also the case for the GlyR, for both the native GlyR of the spinal cord neurons [2] and the heterologously expressed receptors in *Xenopus* oocyte [[6]; see also discussion in [5]]. Therefore, we may assume that in our expression experiments the structure of the GlyR was also conserved. The present results then suggest that for the high-affinity GlyR the narrow constriction of the open channel pore is larger than for the low-affinity GlyR. The gating of the channel was also changed for the high-affinity GlyR as reflected by the increased sensitivity to voltage of the open probability of the channel. Recently, permeation and gating have been shown to be coupled [17] and in the model proposed for the NMDA receptor the conformational changes of the channel modify its accessibility to the permeant ion [17,18]. Such conformational changes may be induced in our condition at high receptor density, by interactions between neighboring receptors. Considering the molecular model of channel opening postulated for the nicotinic acetylcholine receptor by Unwin [19] the rotation of the channel-forming transmembrane peptides may be facilitated at high receptor density.

Acknowledgements: We thank Drs. A. Feltz for supporting this work, help and critical reading of the manuscript, H. Betz for providing the plasmid construct and Y. Maulet for plasmid amplification.

References

[1] Betz, H. (1992) Quart. Rev. Biophys. 25, 381–394.
[2] Langosch, D., Thomas, L. and Betz, H. (1988) Proc. Natl. Acad. Sci. USA 85, 7394–7398.
[3] Schmieden, V., Grenninglogh, G., Schofield, P.R. and Betz, H. (1989) EMBO J. 8, 695–700.
[4] Sontheimer, H., Becker, C.M., Pritchett, D.B., Schofield, P.R., Grenninglogh, G., Kettenmann, H., Betz, H. and Seeburg, P.H. (1989) Neuron 2, 1491–1497.
[5] Taleb, O. and Betz, H. (1994) EMBO J. 13, 1318–1324.
[6] Kuhse, J., Laube, B., Magalei, D. and Betz, H. (1993) Neuron 11, 1049–1056.
[7] Grenninglogh, G., Pribilla, I., Prior, P., Multhaup, G., Beyreuther, K., Taleb, O. and Betz, H. (1990) Neuron 4, 963–970.
[8] Pribilla, I., Tagaki, T., Langosch, D., Bormann, J. and Betz, H. (1992) EMBO J. 11, 4305–4311.
[9] Rundström, N., Schmieden, V., Betz, H., Bormann, J. and Langosch, D. (1994) Proc. Natl. Acad. Sci. USA 91, 8950–8954.
[10] Curtis, D.R. and Johnson, G.A.R. (1974) Rev. Physiol. 69, 96–188.
[11] Grenningloh, G., Schmieden, V., Schofield, P.R., Seeburg, P.H., Siddique, T., Mohandas, T.K., Becker, C.-M. and Betz, H. (1990) EMBO J. 9, 771–776.
[12] Taleb, O., Trouslard, J., Demeneix, B.A., Feltz, P., Bossu, J.-L., Dupont, J.-L. and Feltz, A. (1987) Pflügers Arch. 409, 620–631.
[13] Bormann, J., Hamill, O.P. and Sakmann, B. (1987) J. Physiol. (Lond.) 385, 243–286.
[14] Jentsch, T.J. (1996) Curr. Opin. Neurobiol. 6, 303–310.
[15] Fatima-Shad, K. and Barry, P.H. (1993) Proc. R. Soc. Lond. B 253, 69–75.
[16] Rodeau, J.L. and Vilain, J.P. (1987) Dev. Biol. 120, 481–493.
[17] Schneggenburger, R. and Ascher, P. (1997) Neuron 18, 167–177.
[18] Laüger, P. (1985) Biophys. J. 47, 581–591.
[19] Unwin, N. (1995) Nature 373, 37–43.